

Mathematical Morphology View of Topological Rough Sets and Its Applications

Ibrahim Noaman¹, Abd El Fattah El Atik², Tamer Medhat^{3,*} and Manal E. Ali⁴

¹Department of Mathematics, Faculty of Science and Arts in Al-Mandaq, Al-Baha University, Kingdom of Saudi Arabia

²Department of Mathematics, Faculty of Science, Tanta University, Tanta, Egypt

³Department of Electrical Engineering, Faculty of Engineering, Kafrelsheikh University, Kafrelsheikh, 33516, Egypt

⁴Department of Physics and Engineering Mathematics, Faculty of Engineering, Kafrelsheikh University, Kafrelsheikh, 33516, Egypt

*Corresponding Author: Tamer Medhat. Email: tmedhatm@eng.kfs.edu.eg

Received: 20 June 2022; Accepted: 20 October 2022

Abstract: This article focuses on the relationship between mathematical morphology operations and rough sets, mainly based on the context of image retrieval and the basic image correspondence problem. Mathematical morphological procedures and set approximations in rough set theory have some clear parallels. Numerous initiatives have been made to connect rough sets with mathematical morphology. Numerous significant publications have been written in this field. Others attempt to show a direct connection between mathematical morphology and rough sets through relations, a pair of dual operations, and neighborhood systems. Rough sets are used to suggest a strategy to approximate mathematical morphology within the general paradigm of soft computing. A single framework is defined using a different technique that incorporates the key ideas of both rough sets and mathematical morphology. This paper examines rough set theory from the viewpoint of mathematical morphology to derive rough forms of the morphological structures of dilation, erosion, opening, and closing. These newly defined structures are applied to develop algorithm for the differential analysis of chest X-ray images from a COVID-19 patient with acute pneumonia and a health subject. The algorithm and rough morphological operations show promise for the delineation of lung occlusion in COVID-19 patients from chest X-rays. The foundations of mathematical morphology are covered in this article. After that, rough set theory ideas are taken into account, and their connections are examined. Finally, a suggested image retrieval application of the concepts from these two fields is provided.

Keywords: Mathematical morphology; rough set theory; topological spaces; COVID-19



This work is licensed under a Creative Commons Attribution 4.0 International License, which permits unrestricted use, distribution, and reproduction in any medium, provided the original work is properly cited.

Nomenclature**Abbreviations**

RS	Rough Sets
SE	Structure Element
RD	Rough Dilation
RE	Rough Erosion
RC	Rough Closing
RO	Rough Opening

Symbols

\mathbb{Z}	Positive integers
\mathbb{Z}^2	Discrete topological space
E^d	D-dimensional product of E
X, Y	Images as sets of pixels
B	Structure element
τ	Topological space
CL(X)	Closure of X
Int(X)	Interior of X

1 Introduction and Preliminaries

Pawlak's rough set theory [1] is a mathematical tool that is useful for studying uncertain or incomplete data in information systems and is based on the classification of data into Objects [2]. However, Pawlak's definition of equivalence classes of an equivalence relation for the universe set is not valid for all incomplete data, particularly various real-life problems. By studying Pawlak's rough set theory from a topological point of view, Lashin et al. [3] and Salama et al. [4] derived a general relation and observed that most of Pawlak's properties are not held in a general sense. This led to the study of new kinds of rough sets and their applications by many researchers [5–7]. Neighborhood systems and rough sets have recently been used to represent structures, such as self-similar fractals [8] and the human heart [9], with potential applications in physics and medicine, respectively. One of the most important achievements in rough set theory is knowledge reduction in information systems, by which a membership function is used to reduce the data. Pawlak et al. [10] expanded the membership function into an initial rough membership function, while El Atik et al. [11] used this similarity as a membership function. Allam et al. [12] and Salama [13] presented new approaches for basic rough set concepts. In [14], Yao et al. address the problem of overlapping classes in rough sets and introduce object class membership, and in [15] Yu et al. introduce approximations to measure accuracy. Polkowski et al. introduced some of important mechanisms for rough sets in [16,17].

Differential equations and diffusion equations may both be used to simulate many real-world issues in the fields of science and engineering [18]. Recently, four novel mutant SARS-COV-2 strains that are thought to be 70% more lethal than the currently circulating COVID-19 virus were found in several locations [19]. By using a mathematical model, it is crucial to understand the SARS-CoV-2 dynamics in the context of immune surveillance [20]. In the COVID-19 outbreak investigation, asymptomatic transmission of the coronavirus illness and the prediction of infected individuals have become crucial [21]. For biomathematicians and medical professionals, controlling these acute illnesses has been a major priority in recent years [22].

The main aim of the present paper is to study rough set theory from another angle, that is, from the viewpoint of mathematical morphology. Mathematical morphology provides a range of techniques for image processing and analysis based on basic algebraic and geometric principles. Matheron [23] and Serra [24] first introduced the concepts of mathematical morphology, in application to petrography and mineralogy where they studied the physical properties of certain types of rocks. Mathematical morphology has since been explored in some detail (see, e.g., [25–30]) and has been applied in engineering and medicine [31–34]. A new method for scene classification from the remote sensing images is investigated in [35], but diagnosis and testing of COVID-19 chest are investigated in [36,37].

Here we propose new forms of rough morphological structures: rough dilation, rough erosion, rough closing, and rough opening. These forms are defined for application in topological and digital image processing and applied specifically for the delineation of lung occlusion from a chest x-ray of a patient with acute COVID-19 pneumonia.

This article is organized as follows; Section 2 for morphological definitions of roughness and Section 3 introduces the basic properties of rough dilation and rough erosion. Section 4 presents the application of rough morphological structures for differential analysis of chest x-ray images. Finally, Section 5 presents the conclusion and future work.

Throughout this paper \mathbb{Z}^2 denotes a discrete topological space, where \mathbb{Z} is the set of positive integers and $M, B \subseteq \mathbb{Z}^2$. Also, \mathcal{U} is a nonempty finite universe set, \mathcal{R} is an equivalence relation on \mathcal{U} and $W \subseteq \mathcal{U}$.

Definition 1. [30] Mathematical morphology allows the extraction and analysis of discrete quantal image structures. There are two essential components: the image as a set of objects and a structure element (SE). Each object is represented by binary digits, e.g., (0 = black, 1 = white). Objects are also represented by a coordinate (x, y) in \mathbb{Z}^2 . The SE in \mathbb{Z}^2 is a small set to define the image under study. For each structure element, we define the original shape and size based on the geometric properties of the objects. Examples of SEs are shown in Fig. 1.



Figure 1: Some examples of structure elements

Definition 2. [30] For any two images, $E1$ and $E2$ in the d -dimensional product \mathbb{E}^d of E , Minkowski addition (subtraction) is defined by

$$E1 \oplus E2 = \{e1 + e2: e1 \in E1 \text{ and } e2 \in E2\};$$

$$E1 \ominus E2 = \{h: e2 + h \in E1 \forall e2 \in E2\}.$$

Note that \oplus is commutative and \ominus is not. Any fixed set A in \mathbb{E}^d is said to be a structural element.

Definition 3. [30] The dilation of image called X by structure element called A is given by $\delta_A(X) = X \oplus A$ and the erosion of X by A is $\varepsilon_A(X) = X \ominus A$.

Definition 4. [1] Let (U, R) be a Pawlak’s approximation space. A lower approximation, upper approximation, and boundary region of X by R is defined by

$$L_{\mathcal{R}}(X) = \bigcup_{x \in \mathcal{U}} \{\mathcal{R}(x): \mathcal{R}(x) \subseteq X\},$$

$$U_{\mathcal{R}}(X) = \bigcup_{x \in \mathcal{U}} \{\mathcal{R}(x) : \mathcal{R}(x) \cap X \neq \Phi\},$$

$$B_{\mathcal{R}}(X) = U_{\mathcal{R}}(X) - L_{\mathcal{R}}(X).$$

where $\mathcal{R}(x)$ is the equivalence class for x according to relation \mathcal{R} .

2 Morphological Definitions of Roughness

Dilation and erosion are basic concepts in mathematical morphology and image processing, where any image set X can be dilated (eroded) by a structure element B . Here, we consider rough set theory by scanning \mathbb{Z}^2 through a structure element with the image set, affording new definitions of rough dilation, rough erosion, rough closing, and rough opening. Below and red pixels are denoted by scan cells, and yellow pixels are denoted by the neighborhoods of red pixels.

Definition 5. A rough dilation (RD) and rough erosion (RE) are defined by

$$RD(X; B) = \{x \in \mathbb{Z}^2 : B \cap X \neq \Phi\}, \text{ and}$$

$$RE(X; B) = \{x \in \mathbb{Z}^2 : B \subset X\}, \text{ for } X, B \subset \mathbb{Z}^2.$$

It is clear that $X \subseteq RD(X; B)$ and $RE(X; B) \subseteq X$.

Example 1. Move and scan B_1 in \mathbb{Z}^2 (see Fig. 2b) through its red pixel. By applying Definition 5, we have a rough dilation set as in Fig. 2c.

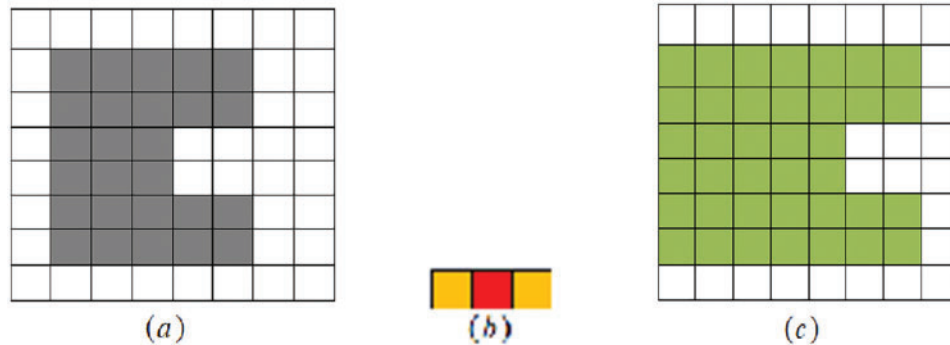


Figure 2: (a) Original image X_1 , (b) The SE B_1 , and (c) the result of processing

Example 2. Move and scan B_2 in \mathbb{Z}^2 (see Fig. 3b) through its red pixel. By applying Definition 5, we have a rough erosion set in Fig. 3c.

Definition 6. Let X and B be subsets of a discrete space \mathbb{Z}^2 . The rough closing (RC) and rough opening (RO) of X by B are given by

$$RC(X; B) = RE(RD(X; B); B) = \bigcup \{p \in \mathbb{Z}^2 : B \subseteq (RD(X; B))\}, \text{ and}$$

$$RO(X; B) = RD(RE(X; B); B) = \bigcup \{p \in \mathbb{Z}^2 : B \cap (RE(X; B)) \neq \Phi\}.$$

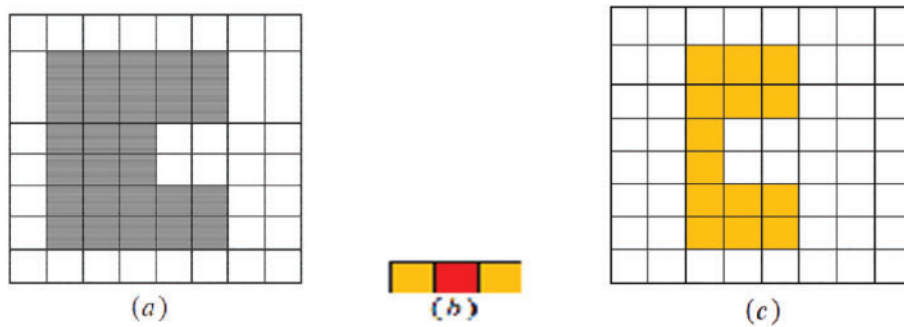


Figure 3: (a) Original image X_2 , (b) The SE B_2 , and (c) the result of processing

Example 3. Move and scan B_1 in \mathbb{Z}^2 (see Fig. 4b) through its red pixel. By applying Definition 6, we have a rough closing set in Fig. 4d.

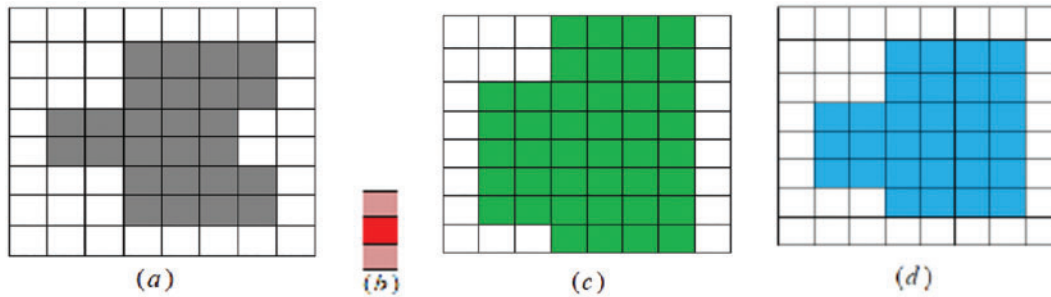


Figure 4: (a) Original image X_1 , (b) B_1 is SE, (c) $RD(X_1; B_1)$ and (d) $RC(X_1; B_1)$

Example 4. Move and scan B_2 in \mathbb{Z}^2 (see Fig. 5b) through its red pixel, by applying Definition 6, we have a rough opening set in Fig. 5d.

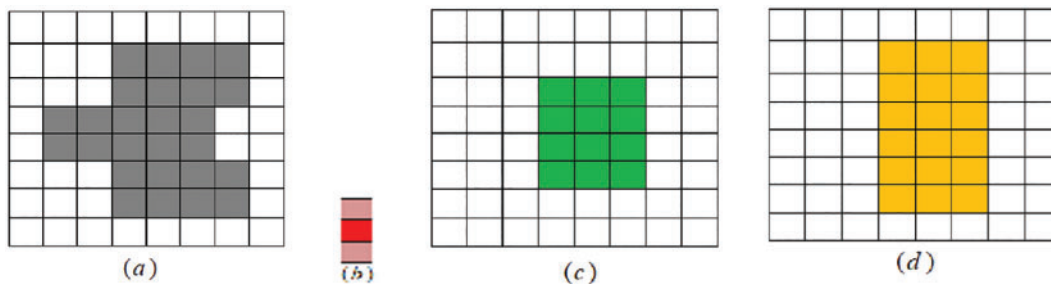


Figure 5: (a) Original image X_2 , (b) The SE B_2 , (c) $RE(X_2; B_2)$ and (d) $RO(X_2; B_2)$

3 Basic Properties of Rough Dilation and Rough Erosion

In this section, we consider some topological properties based on rough dilations and rough erosions. In a topological space \mathbb{Z}^2 , the closure Cl of X ($Cl_{RD}(X; B)$) is the smallest rough dilation of X by B containing X . The interior Int of X ($Int_{RD}(X; B)$) is the largest rough erosion of X by B contains X . Cl and Int denote the closure and interior, respectively, with respect to a topological

space (\mathbb{Z}^2, τ) . In Lemma 1 below, it is easier to prove the relationship between $RD(X; B)$, $RD(Y; B)$, $RE(X; B)$ and $RE(Y; B)$, and so the proof is omitted.

Lemma 1. Let X and Y be image sets in \mathbb{Z}^2 such that $X \subseteq Y$, and let B be a structure element. Then, the following hold:

$$RD(X; B) \subseteq RD(Y; B).$$

$$RE(X; B) \subseteq RE(Y; B).$$

Proposition 1. Let X be an image set and B_1, B_2 be structure elements such that $B_1 \subseteq B_2$. Then, $RD(X; B_1) \subseteq RD(X; B_2)$.

Proof. Let $x \in RD(X; B_1)$. Then, $x \in \mathbb{Z}^2: B_1 \cap X \neq \Phi$, while $B_1 \subseteq B_2$. Therefore, $B_2 \cap X \neq \Phi$, and so $x \in RD(X; B_2)$. Hence, $RD(X; B_1) \subseteq RD(X; B_2)$.

Proposition 2. Let $X \subseteq \mathbb{Z}^2$ and B_1, B_2 be structure elements. Then, the following hold:

$$X \subseteq RD(X; B_1).$$

$$RD(X; B_1) \subseteq RD(RD(X; B_1)).$$

$$RD(X; B_1 \cup B_2) = RD(X; B_1) \cup RD(X; B_2).$$

$$RD(X; B_1 \cap B_2) \subseteq RD(X; B_1) \cap RD(X; B_2).$$

Proof. From Proposition 1, it is easy to prove (i) and (ii).

Let $x \in (X; B_1 \cup B_2) \Rightarrow x \in \mathbb{Z}^2: X \cap (B_1 \cup B_2) \neq \Phi \Rightarrow ((X \cap B_1) \cup (X \cap B_2)) \neq \Phi \Rightarrow X \cap B_1 \neq \Phi$ or $X \cap B_2 \neq \Phi \Rightarrow x \in ((RD(X; B_1) \cup RD(X; B_2))$. Then, $RD(X; B_1 \cup B_2) \subseteq (RD(X; B_1) \cup RD(X; B_2))$. Conversely, let $x \in (RD(X; B_1) \cup RD(X; B_2))$. Then, $x \in (RD(X; B_1)$ or $x \in (RD(X; B_2) \Rightarrow (X \cap B_1) \neq \Phi \cup (X \cap B_2) \neq \Phi \Rightarrow (X \cap (B_1 \cup B_2)) \neq \Phi \Rightarrow x \in RD(X; B_1 \cup B_2)$. So, $(RD(X; B_1) \cup RD(X; B_2)) \subseteq RD(X; B_1 \cup B_2)$. Therefore, $RD(X; B_1 \cup B_2) = RD(X; B_1) \cup RD(X; B_2)$.

Let $x \in RD(X; B_1 \cap B_2) \Rightarrow x \in \mathbb{Z}^2: X \cap (B_1 \cap B_2) \neq \Phi \Rightarrow (X \cap B_1) \neq \Phi$ and $(X \cap B_2) \neq \Phi \Rightarrow x \in RD(X; B_1)$ and $x \in RD(X; B_2)$. Therefore, $RD(X; B_1 \cap B_2) \subseteq RD(X; B_1) \cap RD(X; B_2)$.

Proposition 3. Let X be an image set and B_1, B_2 be structures such that $B_1 \subseteq B_2$. Then, $RE(X; B_2) \subseteq RE(X; B_1)$.

Proof. Let $x \in RE(X; B_2)$. Then, $x \in \mathbb{Z}^2: B_2 \subseteq X$, while $B_1 \subseteq B_2 \Rightarrow B_1 \subseteq X \Rightarrow x \in RE(X; B_1)$. Therefore, $RE(X; B_2) \subseteq RE(X; B_1)$.

Proposition 4. Let $X \subseteq \mathbb{Z}^2$ and B_1, B_2 be structure elements. Then, the following statements hold:

$$RE(X; B_1) \subseteq X.$$

$$RE(RE(X; B_1)) \subseteq RE(X; B_1).$$

$$RE(X; B_1) \cup RE(X; B_2) \subseteq RE(X; B_1 \cup B_2).$$

Proof. From Proposition 3, it is easy to prove (i) and (ii).

Let $x \in (RE(X; B_1) \cup RE(X; B_2))$. Then, $x \in RE(X; B_1)$ or $x \in RE(X; B_2) \Rightarrow x \in \mathbb{Z}^2: B_1 \subseteq X$ or $B_2 \subseteq X \Rightarrow x \in \mathbb{Z}^2: (B_1 \cup B_2) \subseteq X \Rightarrow x \in RE(X; B_1 \cup B_2)$. Therefore, $RE(X; B_1) \cup RE(X; B_2) \subseteq RE(X; B_1 \cup B_2)$.

Remark 1. One can easily note that $RE(X; B_1) \cap RE(X; B_2) \subseteq RE(X; B_1 \cap B_2)$, while $RE(X; B_1 \cap B_2) \not\subseteq RE(X; B_1) \cap RE(X; B_2)$. This can be illustrated as in Example 5.

Example 5. Move and scan B_1 in \mathbb{Z}^2 through its red pixel (see Fig. 6b). Then, we have $RE(X; B_1)$ in Fig. 6c. In the same manner, by using Fig. 6d, we obtain $RE(X; B_2)$ in Fig. 6e. Similarly, move and scan $B_1 \cap B_2$ through its red pixel (see Fig. 6f), we get $RE(X; B_1 \cap B_2)$ in Fig. 6g. By the moving and scanning of $RE(X; B_1)$ in Figs. 6c and 6e $RE(X; B_2)$, we obtain $RE(X; B_1 \cap RE(X; B_2))$ in Fig. 6h.

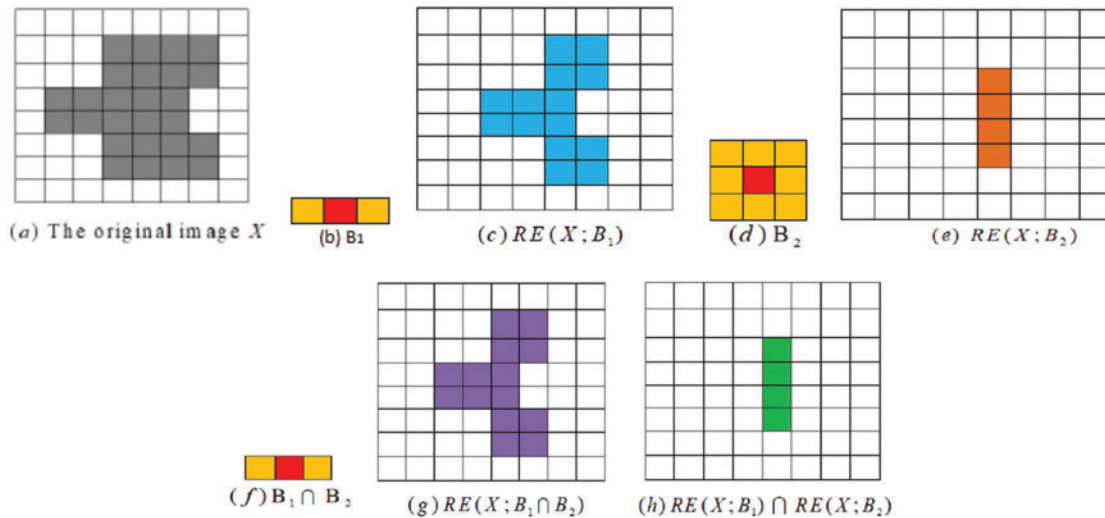


Figure 6: (a) The original image, (b) Structure element B_1 , (c) $RE(X; B_1)$, (d) Structure element B_2 , (e) $RE(X; B_2)$, (f) Structure element $(B_1 \cap B_2)$, (g) $RE(X; B_1 \cap B_2)$ and (h) $RE(X; B_1) \cap RE(X; B_2)$

Proposition 5. The following properties hold $\forall X_1, X_2 \in \mathbb{Z}^2$:

If $X = X_1 \cup X_2$, then $RD(X; B) = RD(X_1; B) \cup RD(X_2; B)$.

If $X = X_1 \cap X_2$, $RD(X; B) = RD(X_1; B) \cap RD(X_2; B)$.

Proof. It is sufficient to prove only (i), as (ii) holds by similarity. As $x \in RD(X; B)$, then $x \in \mathbb{Z}^2: X \cap B \neq \Phi$, while $X = X_1 \cup X_2$. Hence, $(X_1 \cap B) \neq \Phi$ or $(X_2 \cap B) \neq \Phi \Leftrightarrow x \in (RD(X_1; B) \cup RD(X_2; B))$. So, $RD(X; B) = RD(X_1; B) \cup RD(X_2; B)$. On the other hand, with $x \in RD(X; B) \Leftrightarrow x \in \mathbb{Z}^2: X \cap B \neq \Phi$, and $X = X_1 \cap X_2$, we obtain $(X_1 \cap B) \neq \Phi$ and $(X_2 \cap B) \neq \Phi \Leftrightarrow x \in (RD(X_1; B) \cap RD(X_2; B))$. Therefore, $RD(X; B) = RD(X_1; B) \cap RD(X_2; B)$.

Corollary 1. The following properties are held, $\forall X_1, X_2, \dots, X_n \in \mathbb{Z}^2$

If $X = X_1 \cup X_2 \cup \dots \cup X_n$, then $RD(X; B) = RD(X_1; B) \cup RD(X_2; B) \cup \dots \cup RD(X_n; B)$.

If $X = X_1 \cap X_2 \cap X_3 \cap \dots \cap X_n$, then $RD(X; B) = RD(X_1; B) \cap RD(X_2; B) \cap RD(X_3; B) \cap \dots \cap RD(X_n; B)$.

Proposition 6. The following properties hold $\forall X_1, X_2 \in \mathbb{Z}^2$:

If $X = X_1 \cup X_2$, then $RE(X; B) = RE(X_1; B) \cup RE(X_2; B)$.

If $X = X_1 \cap X_2$, then $RE(X; B) = RE(X_1; B) \cap RE(X_2; B)$.

Proof. As $x \in RE(X; B)$, then $x \in \mathbb{Z}^2: B \subseteq X$, while $X = X_1 \cup X_2$. So, $B \subseteq X_1$ or $B \subseteq X_2 \Leftrightarrow x \in (RE(X_1; B) \cup RE(X_2; B))$. Then, $RE(X; B) = RE(X_1; B) \cup RE(X_2; B)$. Similarly, as $x \in RE(X; B)$,

then $x \in \mathbb{Z}^2: B \subseteq X$. But $X = X_1 \cap X_2$. Hence, $B \subseteq X_1$ and $B \subseteq X_2 \Leftrightarrow x \in (RE(X_1; B) \cap RE(X_2; B))$. Therefore, $RE(X; B) = RE(X_1; B) \cap RE(X_2; B)$.

Corollary 2. The following properties hold $\forall X_1, X_2, \dots, X_n \in \mathbb{Z}^2$:

If $X = X_1 \cup X_2 \cup X_3 \cup \dots \cup X_n$, then $RE(X; B) = RE(X_1; B) \cup RE(X_2; B) \cup RE(X_3; B) \cup \dots \cup RE(X_n; B)$.

If $X = X_1 \cap X_2 \cap X_3 \cap \dots \cap X_n$, then $RE(X; B) = RE(X_1; B) \cap RE(X_2; B) \cap RE(X_3; B) \cap \dots \cap RE(X_n; B)$.

Proposition 7. Let X and Y be image sets. The following hold:

$$RE(X) \subseteq X \subseteq RD(X).$$

$$RE(\Phi) = RD(\Phi) = \Phi.$$

$$RD(X \cup Y) = RD(X) \cup RD(Y).$$

$$RE(X \cap Y) = RE(X) \cap RE(Y).$$

$$RE(X \cup Y) \supset RE(X) \cap RE(Y).$$

$$X \subseteq Y \Rightarrow RD(X) \subseteq RD(Y).$$

$$X \subseteq Y \Rightarrow RE(X) \subseteq RE(Y).$$

Proof. By Propositions 1 and 3, proofs of (i) and (ii) are obvious.

Since $X \subseteq (X \cup Y) \Rightarrow RD(X) \subseteq RD(X \cup Y)$ and $Y \subseteq (X \cup Y)$, then $RD(Y) \subseteq RD(X \cup Y)$, and so $RD(X) \cup RD(Y) \subseteq RD(X \cup Y)$. On the other hand, let $x \in RD(X \cup Y)$. Then, by rough dilation, $x \in \mathbb{Z}^2: B \cap (X \cup Y) \neq \Phi$ and so $(B \cap X) \cup (B \cap Y) \neq \Phi$. Hence, $(B \cap X) \neq \Phi$ or $(B \cap Y) \neq \Phi$ and so $x \in RD(X) \cup RD(Y)$. Then, $RD(X \cup Y) \subseteq RD(X) \cup RD(Y)$. Therefore, $RD(X \cup Y) = RD(X) \cup RD(Y)$.

Since $X \cap Y \subseteq X$, then $RE(X \cap Y) \subseteq RE(X)$ and $X \cap Y \subseteq Y$, and so $RE(X \cap Y) \subseteq RE(Y)$. Hence, $RE(X \cap Y) \subseteq RE(X) \cap RE(Y)$. Conversely, let $x \in RE(X) \cap RE(Y)$. By rough erosion, $x \in \mathbb{Z}^2: B \subseteq X \cap Y$ and so $x \in RE(X)$ and $x \in RE(Y)$, $x \in \mathbb{Z}^2: B \subseteq X$ and $x \in \mathbb{Z}^2: B \subseteq Y \Rightarrow x \in \mathbb{Z}^2: B \subseteq X \cap Y \rightarrow x \in RE(X \cap Y)$, giving $RE(X) \cap RE(Y) \subseteq RE(X \cap Y)$. Thus, $RE(X \cap Y) = RE(X) \cap RE(Y)$.

Since $X \subset X \cup Y$, then $RE(X) \subset RE(X \cup Y)$ and $Y \subset X \cup Y \Rightarrow RE(Y) \subset RE(X \cup Y)$, giving $RE(X \cup Y) \supset RE(X) \cap RE(Y)$.

Let $x \in RD(X)$. Then, $B \cap X \neq \Phi$. Since $X \subseteq Y \Rightarrow B \cap X \neq \Phi$, then $x \in RD(Y)$, and so $RD(X) \subseteq RD(Y)$.

Let $x \in RE(X)$. Then, $B \subseteq X$. Since $X \subseteq Y$, then $B \subseteq Y$, and so $x \in RE(Y)$. Therefore, $RE(X) \subseteq RE(Y)$.

Remark 2 shows that the equalities do not hold in general. This can be seen from Examples: example 6, example 7 and example 8.

Remark 2. Let X and Y be image sets in \mathbb{Z}^2 . Then

- (i) $RE(\mathbb{Z}^2) \neq RD(\mathbb{Z}^2) \neq \mathbb{Z}^2$.
- (ii) $RD(X \cup Y) \not\subseteq RD(X) \cap RD(Y)$.
- (iii) $RE(X^c) \neq (RD(X))^c$.
- (iv) $RD(X^c) \neq (RE(X))^c$.
- (v) $RE(RE(X)) \neq RD(RE(X)) \neq RE(X)$.
- (vi) $RD(RD(X)) \neq RE(RD(X)) \neq RD(X)$.

Example 6. Let B in Fig. 7b move and scan in \mathbb{Z}^2 through its red pixel. From Remark 2 (ii), we have Fig. 7c. Also, from Fig. 7d we have $RD(X \cup Y) \not\subseteq RD(X) \cap RD(Y)$.

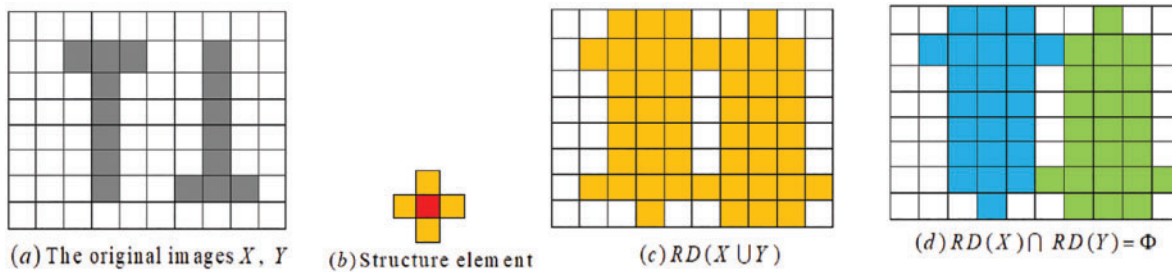


Figure 7: (a) The original images X and Y , (b) Structure element, (c) $RD(X \cup Y)$, and (d) $RD(X) \cap RD(Y)$

Example 7. Let B in Fig. 8b move and scan in \mathbb{Z}^2 through its red pixel. From Remark 2 (iii) and (iv), we have Fig. 8d. Also, from Fig. 8f we have $RE(X^c) \neq (RD(X))^c$.

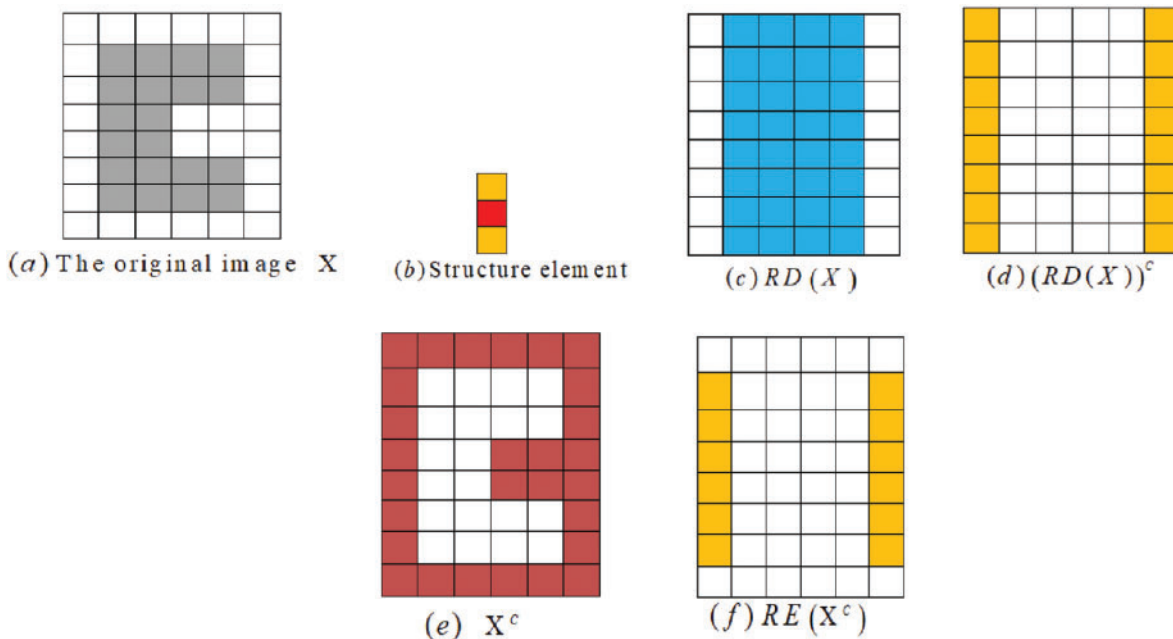


Figure 8: (a) The original image X , (b) Structure element, (c) $RD(X)$, (d) $(RD(X))^c$, (e) X^c , and (f) $RE(X^c)$

The property (iv) in Remark 2 can also be seen to be satisfied in Example 8.

Example 8. Let B in Fig. 9b be a move and scan in \mathbb{Z}^2 through its red pixel. By Remark 2 (v) and (vi), we have Figs. 9c–9e. Hence, $RE(RE(X)) \neq RD(RE(X)) \neq RE(X)$.

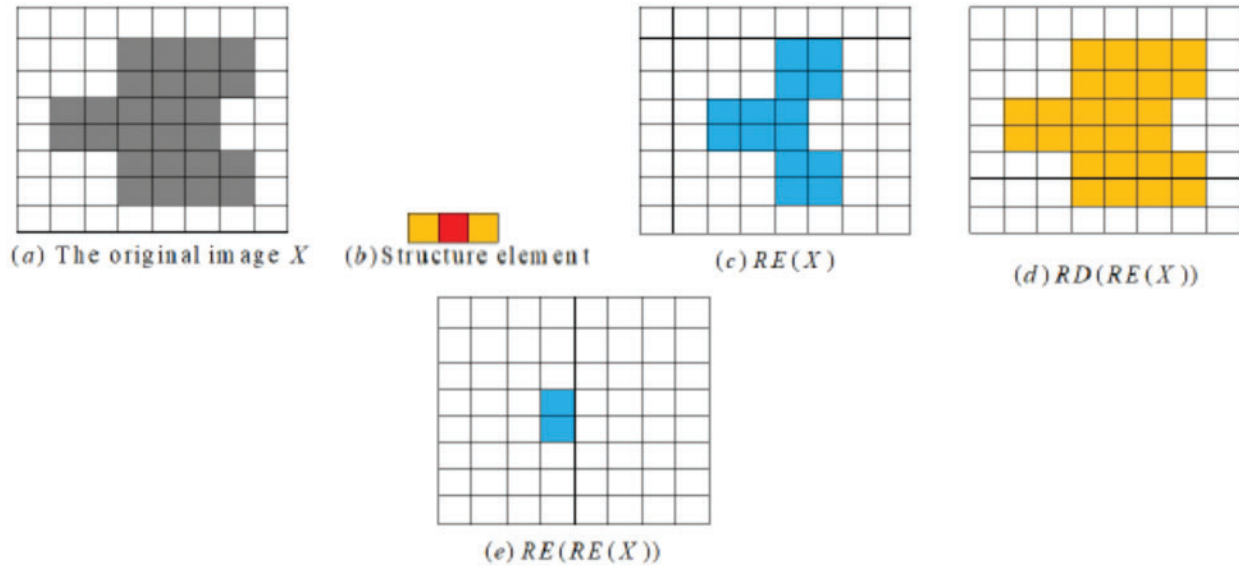


Figure 9: (a) The original image X , (b) Structure element, (c) $RE(X)$, (d) $RD(RE(X))$, and (e) $RE(RE(x))$

Proposition 8. Let X and Y be images in \mathbb{Z}^2 . Then, $RE(X) \cup RE(Y) \subseteq RE(X \cup Y)$.

Proof. Since $X \subseteq (X \cup Y)$, then $RE(X) \subseteq RE(X \cup Y)$ and $Y \subseteq (X \cup Y)$. Hence, $RE(Y) \subseteq RE(X \cup Y)$ and so $RE(X) \cup RE(Y) \subseteq RE(X \cup Y)$.

Proposition 9. Let X and Y be images in \mathbb{Z}^2 . Then, $RD(X \cap Y) \subseteq RD(X) \cup RD(Y)$.

Proof. Since $(X \cap Y) \subseteq X$, then $RD(X \cap Y) \subseteq RD(X)$ and $(X \cap Y) \subseteq Y$. Hence, $RD(X \cap Y) \subseteq RD(Y)$ and so $RD(X \cap Y) \subseteq RD(X) \cup RD(Y)$.

4 Application of Rough Morphological Structures for Differential Analysis of Chest X-ray Images

One of the symptoms of severe SARS-CoV-2 coronavirus diseases [38] is the development of pneumonia and acute respiratory distress syndrome (ARDS) [39]. Admitted patients suspected of such severe COVID-19 disease typically undergo a radiological examination of the lungs for ARDS. While computed tomography offers the most sensitive and accurate imaging of lung condition [40,41], chest X-rays are often the front-line approach employed by many hospitals and can be performed using portable equipment [42], which can reduce patient movements and thereby lower the risk of infection [43–45]. The importance of chest X-ray imaging for the diagnosis of ARDS in COVID-19 pneumonia prompted us to examine whether rough morphological structures could be used to aid differential diagnostics.

Figs. 10 and 11 show two typical chest X-ray images, one from a health subject and another from a COVID-19 patient with ARDS.

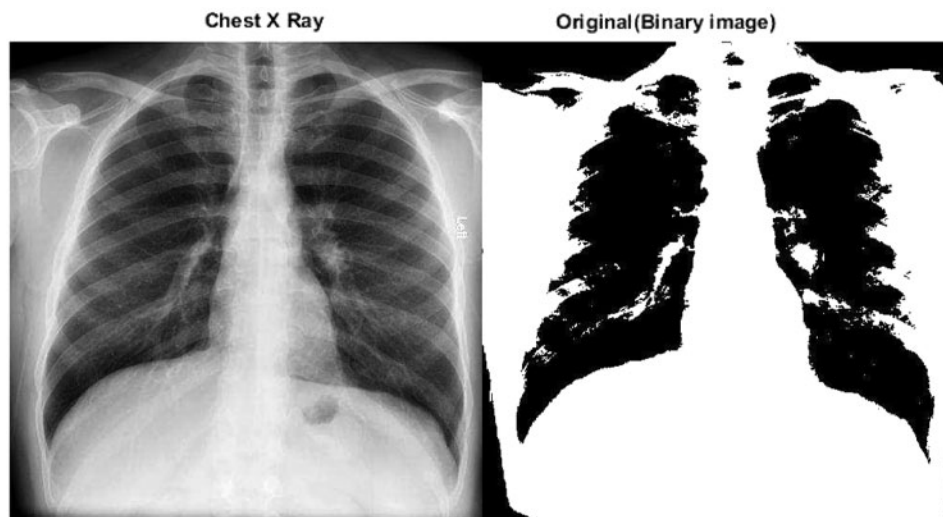


Figure 10: A chest X-ray of a COVID-19 patient with ARDS and the corresponding binary image in \mathbb{Z}^2

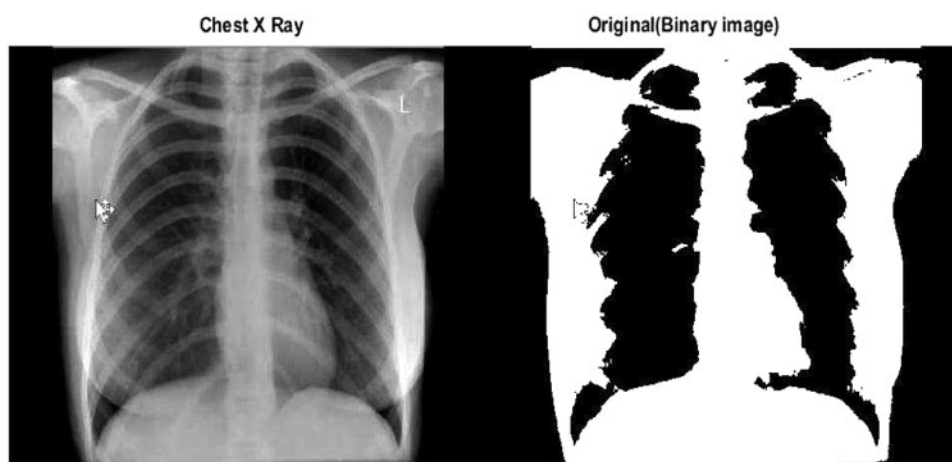


Figure 11: A chest X-ray of a healthy subject and corresponding binary image in \mathbb{Z}^2

Now we consider the rough boundary (rough opening and rough closing) using the original-rough opening and rough closing–original transforms, as shown in [Figs. 12](#) and [13](#).

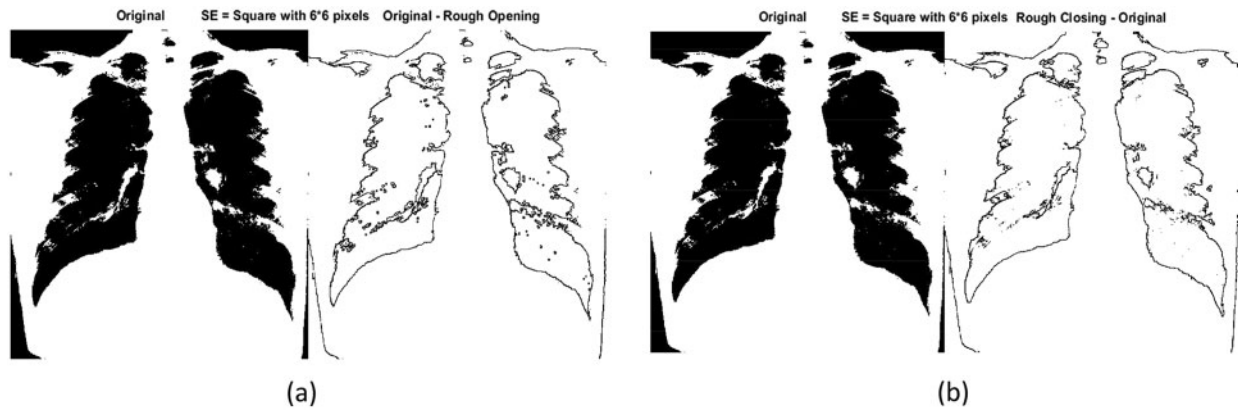


Figure 12: (a) Original-rough opening transform for the chest X-ray of a COVID-19 patient in \mathbb{Z}^2 (b) Rough closing-original transform for chest X-ray of a COVID-19 patient in \mathbb{Z}^2

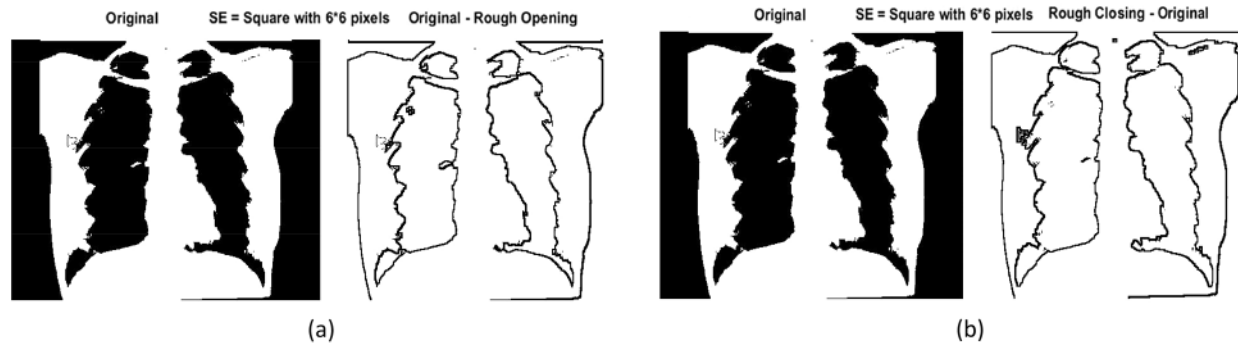


Figure 13: (a) Original-rough opening transform for the chest X-ray of a healthy subject in \mathbb{Z}^2 (b) Rough closing-original transform for chest X-ray of a healthy subject in \mathbb{Z}^2

An algorithm for differential analysis of these two images is provided below: algorithm 1. Here, RD and RE are operators. The input image is the binary image of the chest X-ray (image 1; IM1) with size p ($xmax, ymax$), and we use square 3×3 pixels as structural elements (B). The algorithm stores the result in image 2 (IM2) for rough dilation and image 3 (IM3) for rough erosion.

Algorithm 1: Rough dilation (RD) and rough erosion (RE) on chest x-ray images

Input: Chest X-ray image as a binary image (IM1), structure element $B =$ square of 3×3 pixels

Output: RD and RE of IM1 as IM2 and IM3, respectively.

Step 1: IM1 = imread('chest X-ray.png'); //Read chest X-ray image as binary image IM1.

Step 2: P = size(IM1); //Calculate the size of IM1.

Step 3: B = [1 1 1; 1 1 1; 1 1 1]; // Put $B =$ square of 3×3 pixels.

Step 4:

For x = 2: 1: P(1) - 1 do

For y = 2: 1: P(2) - 1 do

T1 = [B(1) * IM1(x - 1, y - 1)	B(2) * IM1(x - 1, y)	B(3) * IM1(x - 1, y + 1);
B(4) * IM1(x, y - 1)	B(5) * IM1(x, y)	B(6) * IM1(x, y + 1);
B(7) * IM1(x + 1, y - 1)	B(8) * IM1(x + 1, y)	B(9) * IM1(x + 1, y + 1)]

(Continued)

Algorithm 1: Continued

$$IM2(x, y) = \max(T1); // \text{Rough dilation}$$

$$IM3(x, y) = \min(T1); // \text{Rough erosion}$$

End

End

Step 5: Display figure(1), imshow(IM2); //Display the rough dilation of image IM1.**Step 6:** Display figure(2), imshow(IM3); //Display the rough erosion of image IM1.

The main steps for finding the rough opening (RO) and rough closing (RC) of the chest X-ray images are shown in the following flowchart at [Fig. 14](#).

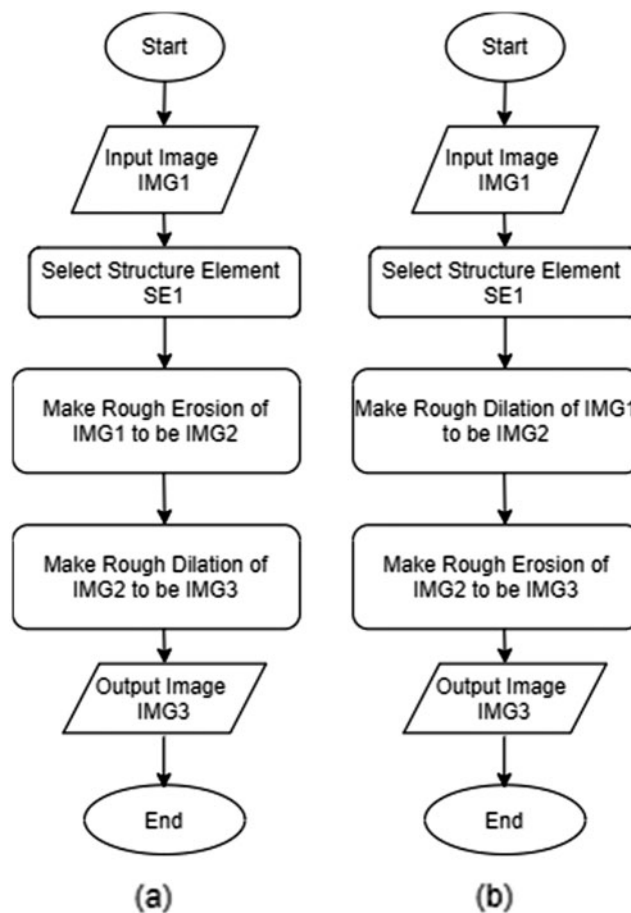


Figure 14: Flowchart of (a) rough opening and (b) rough closing on chest X-ray images

5 Conclusion and Future Work

Although mathematical morphology and rough set theory are two different fields in terms of their initial domains and implementations, there are relations between the two systems as shown in this article. Specifically, we have shown that the lower and upper approximations of rough set theory are similar to opening/erosion and closing/dilation in mathematical morphology. This principle can

be used to find similarity among images with a lower approximation. The topology of the partition can be defined in images as part of the universe set using four features defined using color and image indices. Subspace topologies can also be used to model each image type. We proposed an algorithm using these rough morphological operations that could be used to delineate lung occlusion (ARDS) in COVID-19 patients from chest X-ray images. In future work, we will add the detection accuracy measured.

Authors' Contributions: All authors read and approved the final manuscript.

Availability of Data and Materials: The datasets used and analyzed during the current study are public and available from the corresponding author on request.

Funding Statement: The authors received no specific funding for this study.

Conflicts of Interest: The authors declare that they have no conflicts of interests to report regarding the present study.

References

- [1] Z. Pawlak, "Rough sets," *International Journal of Information and Computer Sciences*, vol. 11, pp. 341–356, 1982.
- [2] Z. Pawlak, "Rough sets: Theoretical aspects of reasoning about data," *Springer Science & Business Media*, vol. 9, 2012.
- [3] E. F. Lashin, A. M. Kozae, A. A. Abo Khadra and T. Medhat, "Rough set theory for topological spaces," *International Journal of Approximate Reasoning*, vol. 40, no. 1–2, pp. 35–43, 2005.
- [4] A. S. Salama and O. G. El-Barbary, "Topological approach to retrieve missing values in incomplete information systems," *Journal of the Egyptian Mathematical Society*, vol. 25, no. 4, pp. 419–423, 2017.
- [5] A. Ahmad, U. Qamar and M. S. Raza, "An optimized method to calculate approximations in dominance based rough set approach," *Applied Soft Computing*, vol. 97, pp. 1–13, 2020.
- [6] Z. Huang and J. Li, "Multi-scale covering rough sets with applications to data classification," *Applied Soft Computing*, vol. 110, pp. 107736, 2021.
- [7] P. Zhou, P. Li, S. Zhao and Y. Zhang, "Online early terminated streaming feature selection based on rough set theory," *Applied Soft Computing*, vol. 113, pp. 1–12, 2021.
- [8] A. El Atik and A. Nasef, "Some topological structures of fractals and their related graphs," *Filomat*, vol. 34, no. 1, pp. 153–165, 2020.
- [9] A. El Atik, "Reduction based on similarity and decision-making," *Journal of the Egyptian Mathematical Society*, vol. 28, no. 1, pp. 1–12, 2020.
- [10] Z. Pawlak and A. Skowron, "Rough membership functions," in *Advances in the Dempster-Shafer Theory of Evidence*, vol. 22, New York: John Wiley & Sons, pp. 251–271, 1994.
- [11] A. El Atik and H. Hassan, "Some nano topological structures via ideals and graphs," *Journal of the Egyptian Mathematical Society*, vol. 28, no. 1, paper no. 41, pp. 1–21, 2020.
- [12] A. A. Allam, M. Y. Bakeir and E. A. Abo-Tabl, "New approach for basic rough set concepts," in *Proc. Int. Workshop on Rough Sets, Fuzzy Sets, Data Mining, and Granular-Soft Computing*, Regina, Canada: Springer, pp. 64–73, 2005.
- [13] A. S. Salama, "Some topological properties of rough sets with tools for data mining," *International Journal of Computer Science Issues (IJCSI)*, vol. 8, no. 3, pp. 588–595, 2011.
- [14] Y. Y. Yao and J. P. Zhang, "Interpreting fuzzy membership functions in the theory of rough sets," in *Proc. Int. Conf. on Rough Sets and Current Trends in Computing*, RSCTC 2000 Banff, Canada: Springer, pp. 82–89, 2000.

- [15] Z. Yu and D. Wang, "Accuracy of approximation operators during covering evolutions," *International Journal of Approximate Reasoning*, vol. 117, pp. 1–14, 2020.
- [16] L. Polkowski and A. Skowron. "Rough mereology: A new paradigm for approximate reasoning," *International Journal of Approximate Reasoning*, vol. 15, no. 4, pp. 333–365, 1996.
- [17] A. Skowron and L. Polkowski, "Rough mereological foundations for design, analysis, synthesis, and control in distributed systems," *Information Sciences*, vol. 104, no. 1, pp. 129–156, 1998.
- [18] V. F. Morales-Delgado, J. F. Gómez-Aguilar, K. M. Saad, M. A. Khan and P. Agarwal, "Analytic solution for oxygen diffusion from capillary to tissues involving external force effects: A fractional calculus approach," *Physica A*, vol. 523, pp. 48–65, 2019.
- [19] A. u. Rehman, R. Singh and P. Agarwal, "Modeling, analysis and prediction of new variants of COVID-19 and dengue co-infection on complex network," *Chaos, Solitons & Fractals*, vol. 150, pp. 111008, 2021.
- [20] S. M. E. K. Chowdhury, J. T. Chowdhury, S. F. Ahmed, P. Agarwal, I. A. Badruddin *et al.*, "Mathematical modelling of COVID-19 disease dynamics: Interaction between immune system and SARS-CoV-2 within host," *AIMS Mathematics*, vol. 7, no. 2, pp. 2618–2633, 2022.
- [21] S. M. E. K. Chowdhury, M. Forkan, S. F. Ahmed, P. Agarwal, A. B. M. Shawkat Ali *et al.*, "Modeling the SARS-CoV-2 parallel transmission dynamics: Asymptomatic and symptomatic pathways," *Computers in Biology and Medicine*, vol. 143, pp. 105264, 2022.
- [22] P. Agarwal, J. J. Nieto, M. Ruzhansky and D. F. M. Torres, "Analysis of infectious disease problems (COVID-19) and their global impact," in *Infosys Science Foundation Series*, Singapore: Springer, 2021.
- [23] G. Matheron, *Random Sets and Integral Geometry*. New York: John Wiley and Sons, 1975.
- [24] J. Serra, *Image Analysis and Mathematical Morphology*, vol. 11. London: Academic Press, 1988.
- [25] E. Dougherty, *Mathematical Morphology in Image Processing*. Boca Raton, Florida, USA: CRC Press, 2018.
- [26] C. R. Giardina and E. R. Dougherty, *Image Processing-Continuous to Discrete*. New York: Prentice Hall, 1987.
- [27] C. R. Giardina and E. R. Dougherty, *Morphological Methods in Image and Signal Processing*. New Jersey, USA: Prentice-Hall, 1988.
- [28] S. R. Haralick, R. M. Sternberg and X. Zhuang, "Image analysis using mathematical morphology," *IEEE Transactions on Pattern Analysis and Machine Intelligence*, vol. 4, pp. 532–550, 1987.
- [29] H. J. A. M. Heijmans, *Morphological Image Operators*. Boston: Academic Press, 1994.
- [30] H. J. A. M. Heijmans, "Mathematical morphology: Basic principles," in *Proc. of Summer School on Morphological Image and Signal Processing*, Citeseer, 1995.
- [31] L. Guang, L. Xiaoqiong, T. Jingtian, L. Jin, R. Zhengyong *et al.*, "De-noising low-frequency magnetotelluric data using mathematical morphology_ltering and sparse representation," *Journal of Applied Geophysics*, vol. 172, pp. 103919, 2020.
- [32] B. Jess, O. Peter, V. Luca and M. Martijn, "Mathematical morphology directly applied to point cloud data," *ISPRS Journal of Photogrammetry and Remote Sensing*, vol. 168, pp. 208–220, 2020.
- [33] R. Safdar, R. Tauheed, S. Mazhar and J. Shahzad, "Performance analysis of power system parameters for islanding detection using mathematical morphology," *Ain Shams Engineering Journal*, vol. 2, no. 1, pp. 517–527, 2021.
- [34] T. Zhaonian, J. Weixing, G. Jianhua, Z. Yueyan, B. Akrem *et al.*, "Mmsparse: 2d partitioning of sparse matrix based on mathematical morphology," *Future Generation Computer Systems*, vol. 108, pp. 521–532, 2020.
- [35] P. Kollapudi, S. Alghamdi, N. Veeraiah, Y. Alotaibi, S. Thotakura *et al.*, "A new method for scene classification from the remote sensing images," *Computers, Materials & Continua*, vol. 72, no. 1, pp. 1339–1355, 2022.
- [36] A. Mohammadi, Y. Wang, N. Enshaei, P. Afshar, F. Naderkhani *et al.*, "Diagnosis/prognosis of COVID-19 chest images via machine learning and hypersignal processing: Challenges, opportunities, and applications," *IEEE Signal Processing Magazine*, vol. 38, no. 5, pp. 37–66, 2021.

- [37] Y. Alotaibi and A. F. Subahi, "New goal-oriented requirements extraction framework for e-health services: A case study of diagnostic testing during the COVID-19 outbreak," *Business Process Management Journal*, vol. 28, no. 1, pp. 273–292, 2022.
- [38] N. Chen, M. Zhou, X. Dong, J. Qu, F. Gong *et al.*, "Epidemiological and clinical characteristics of 99 cases of 2019 novel coronavirus pneumonia in Wuhan, China: A descriptive study," *Lancet*, vol. 395, pp. 507–513, 2020.
- [39] A. Giovagnoni, "Facing the COVID-19 emergency: We can and we do," *Radiol. Med.*, vol. 125, no. 4, pp. 337–338, 2020.
- [40] C. Wang, P. W. Horby, F. G. Hayden and G. F. Gao, "A novel coronavirus outbreak of global health concern," *The Lancet*, vol. 395, pp. 470–473, 2020.
- [41] W. Yang, A. Sirajuddin, X. Zhang, G. Liu, Z. Teng *et al.*, "The role of imaging in 2019 novel coronavirus pneumonia (COVID-19)," *European Radiology*, vol. 30, no. 9, pp. 4874–4882, 2020.
- [42] K. F. Haque and A. Abdelgawad, "A deep learning approach to detect COVID-19 patients from chest X-ray images," *AI*, vol. 1, no. 3, pp. 418–435, 2020.
- [43] M. K. El-Bably and A. A. El Atik, "Soft-rough sets and their application to determine COVID-19," *Turkish Journal of Mathematics*, vol. 45, pp. 1133–1148, 2021.
- [44] S. Zhou, Y. Wang, T. Zhu and L. Xia, "Ct features of coronavirus disease 2019 (COVID-19) pneumonia in 62 patients in Wuhan, China," *American Journal of Roentgenology*, vol. 214, no. 6, pp. 1287–1294, 2020.
- [45] N. Zhu, D. Zhang, W. Wang, X. Li, B. Yang *et al.*, "A novel coronavirus from patients with pneumonia in China, 2019," *New England Journal of Medicine*, vol. 382, no. 8, pp. 727–733, 2020.